HEAT AND SALT TRANSFER IN DOUBLE-DIFFUSIVE SYSTEMS

Herbert E. Huppert*

ABSTRACT

This study investigates the two-dimensional finite amplitude motions of a fluid confined between two infinite horizontal planes, and heated and salted from below. By a combination of numerical simulation and perturbation theory, the possible forms of equilibrium motion are calculated for different values of the thermal and saline Rayleigh numbers, the Prandtl number and the ratio of the diffusivities of heat and salt. It is shown that equilibrium motions lie on either an oscillatory branch or a time-independent branch. On the oscillatory branch, the motion can be either periodic or non-periodic. In some parameter ranges, stable motions exist on both branches, which leads to a hysteresis effect. Non-periodic motions evolve into time-dependent states at a critical thermal Rayleigh number, and disordered motion is suppressed by increasing the thermal Rayleigh number beyond this critical value.

INTRODUCTION

Double-diffusive convection is a generic term identifying the form of motion which can occur in a fluid in which there are two components of different molecular diffusivities, which make opposing contributions to the vertical density gradient. Practical applications of this form of convection occur for a large number of different components, and many results in this field have been rediscovered by workers in different research disciplines. The original investigations were concerned with the components heat and salt, relevant to the oceans and to solar ponds, and have now been extended to include components relevant to the storage of liquid gas, the liquifying of metals, and the evolution of stars, to cite only a few examples. References to a variety of applications are contained in the review article by Turner (1). In addition to the many applications of double-diffusive convection, interest in the subject has developed as a result of the marked difference between this form of convection and convection involving only one component, as for example in purely thermal convection. In contrast to thermal convection, motions can arise even when the density decreases with height, that is, when the basic state is statically stable. This is due to the effects of diffusion, which is a stabilizing influence in thermal convection, but can act in a double-diffusive fluid in such a way as to release potential energy stored in one of the components, and convert it into the kinetic energy of the motion.

The physical mechanism underlying one of the fundamental forms of double-diffusive motion can be understood from the following parcel argument. Using the terminology of heat and salt, as we shall throughout this paper, consider a fluid whose temperature, salinity and density all decrease monotonically with

---

*Department of Applied Mathematics and Theoretical Physics, Cambridge, England.

height. If a fluid parcel is raised, it comes into a cooler, less salty and less dense environment. Because the rate of molecular diffusion of heat is larger than that of salt, the thermal field of the parcel tends to equilibrate with its surroundings more rapidly than does the salt field. The parcel is then heavier than its surroundings and sinks. But because of the finite value of the thermal diffusion coefficient, the temperature field of the parcel lags the displacement field, and the parcel returns to its original position heavier than it was at the outset. It then sinks to a depth greater than the original rise, whereupon the above process continues, leading to growing oscillations, or overstability, resisted only by the effects of viscosity. This linear mechanism was first explained by Stern (2). If the temperature gradient is sufficiently large compared to the salinity gradient, non-linear disturbances may exist which lead to monotonic motions, because the large temperature field is then able to overcome the restoring tendency of the salinity field. An evaluation of the conditions under which this monotonic form of motion can occur is one of the aims of the investigation reported in this paper.

The motion in the inverse situation - warmer, saltier fluid overlying relatively colder, fresher fluid - is independent of time and occurs as a result of fluid with downward motion transferring its heat to adjacent rising fluid, much in the manner of a heat exchanger. This form of motion, called salt-fingering because of the long narrow convection cells it produces, was first analysed by Stern (2), and some non-linear aspects have been considered by Straus (3).

THE THEORETICAL MODEL

The traditional geometry in which convective motions have been analysed quantitatively, confines the fluid between two infinite horizontal planes, heated, and in our case also salted, from below. In the purely thermal situation, many of the theoretically determined results have been experimentally verified and successfully used to explain various phenomena, as summarized by Spiegel (4). In the double-diffusive situation, Huppert and Manins (5) develop some theoretical results which predict with a high degree of accuracy the outcome of a series of experiments in which two uniform layers of different solute concentrations were initially separated by a paper-thin horizontal interface. For details, the reader is referred to the original paper. The relevant comment to be made here is that the theoretical model, which incorporates the seemingly constraining presence of horizontal planes, was successfully used in a situation uninfluenced by boundaries.

Turning now to an explicit statement of the model analysed in this paper, consider a fluid which occupies the space between two infinite horizontal planes separated by a distance D. The upper plane is maintained at temperature T_0 and salinity S_0 and the lower plane at temperature $T_0 + \Delta T$ and salinity $S_0 + \Delta S$. Both planes will be considered stress-free and perfect conductors of heat and salt. We restrict attention to two-dimensional motion, dependent only on one horizontal co-ordinate and the vertical co-ordinate. Non-dimensionalising all lengths with respect to D and time with respect to D^2/κ_T, where κ_T is the thermal diffusivity, and expressing the velocity q^*, in terms of a streamfunction ψ by

$$q^* = (\kappa_T/D)\ (\psi_z, -\psi_x) \tag{1}$$

the temperature, T^*, by

$$T^* = T_o + \Delta T(1 - z + T) \tag{2}$$

and the salinity S^*, by

$$S^* = S_o + \Delta S(1 - z + S) \tag{3}$$

we can write the governing Boussinesq equations of motion as

$$\sigma^{-1}\nabla^2\psi_t - \sigma^{-1}J(\psi,\nabla^2\psi) = -R_T\, T_x + R_S\, S_x + \nabla^4\psi \tag{4}$$

$$T_t + \psi_x - J(\psi,T) = \nabla^2 T \tag{5}$$

$$S_t + \psi_x - J(\psi,S) = \tau\nabla^2 S \tag{6}$$

$$\psi = \psi_{zz} = T = S = 0 \qquad (z = 0,1) \tag{7}$$

where the Jacobian, J, is defined by

$$J(f,g) = f_x\, g_z - f_z\, g_x \tag{8}$$

The appropriate vertical boundary condition to be applied to Eqs (4)-(6) is that the solution be periodic in x over a distance L, for a prescribed L. The linear equation of state

$$\rho^* = \rho_o(1 - \alpha T^* - \beta S^*) \tag{9}$$

where α and β are taken to be constant has been assumed in the expressions for the body-force term of Eq. (4). Four non-dimensional parameters appear in Eqs (4)-(6): the Prandtl number $\sigma = \nu/\kappa_T$, where ν is the kinematic viscosity; the ratio of the diffusivities $\tau = \kappa_S/\kappa_T$, where κ_S is the saline diffusivity, which is less than κ_T; the thermal Rayleigh number $R_T = \alpha g\Delta T D^3/(\kappa_T\nu)$, where g is gravity; and the saline Rayleigh number $R_S = \beta g\Delta S D^3/(\kappa_T\nu)$. The first two parameters characterize the fluid, while the last two characterize externally applied parameters of the model. In this paper, both Rayleigh numbers are taken to be positive.

SOLUTIONS

The solutions of the linear problem, obtained by neglecting the quadratic Jacobians in Eqs (4)-(7) are well known; see for example Veronis (6) and Baines and Gill (7). The results of such a linear analysis are shown in Figs 1-3 for specific values of σ and τ and for $L = 2$, which is the value of L for which the various modes of convection first occur. According to linear theory, for fixed R_S greater than R_X of Figs 1-3, as R_T increases, the motion passes successively through regions of: conduction only $(0 < R_T < R_1)$; oscillatory convection of increasing amplitude $(R_1 < R_T < R_C)$; and monotonic convection of increasing amplitude $(R_C < R_T)$. Steady convection, that is, convection of constant amplitude, can occur only if $R_T = R_1$ or $R_T = R_6$. For all practical values of the parameters, R_S is greater than R_X, and only this case is considered here. The linear results, which act as a foundation for a non-linear investigation, are more fully discussed by Turner (8), in a chapter devoted to double-diffusive convection.

The most transparent form in which to express our results is by extending the description in the last paragraph to incorporate the important non-linear effects. In particular, we evaluate the possible non-linear modes for fixed R_S. Results presented here have been obtained in part from direct numerical solution of Eqs (4)-(7) and in part from consideration of the perturbation of Eqs (4)-(7) about the linear solutions. The former has been accomplished by approximating Eqs (4)-(7) by space- and time-centred second-order difference equations in ψ, $\nabla^2\psi$, T and S over a rectangular staggered mesh on the domain $0 < x < L$, $0 < z < 1$. The equations incorporate the conditions $\psi = \psi_{xx} = T_x = S_x = 0$ at $x = 0$ and L. From the equations, values of $\nabla^2\psi$, T and S at the gridpoints are calculated at time $t + \delta t$ from given values at time t. The variable ψ is then calculated from $\nabla^2\psi$ by inverting the Laplacian, using an implicit finite-difference approximation to Poisson's equation. This process is repeated for as many time steps as required. The program is an extension of one used originally by Moore, Peckover and Weiss (9) and further details can be obtained from their paper.

A large number of numerical experiments over a range of values of σ, τ, R_T and R_S have been conducted. From these, the possible forms of motion can be characterized in general terms. This is best accomplished by considering σ, τ and R_S to be fixed and tracing existing equilibrium solutions in an R_T – amplitude plane. The amplitude of any solution is here specified by the horizontally averaged heat and salt transports, or their non-dimensional representations, the thermal and saline Nusselt numbers, evaluated at the lower boundary, $z = 0$. These are given by

$$N_T = 1 - \overline{T}_z\ (z = 0) \quad \text{and} \quad N_S = 1 - \overline{S}_z\ (z = 0) \tag{10}$$

where the overbar denotes a horizontal average.

Equilibrium non-linear solutions must emanate, or bifurcate, from the linear solutions at $R_T = R_1$ or at $R_T = R_6$, and are most easily explained by reference to Fig. 4, which presents the solutions for $\sigma = 1.0$ and $\tau = 10^{-2}$ in an $R_T - N_S$ plane.

<u>The Oscillatory Branch</u>

From $R_T = R_1$ there emanates a solution which is generally supercritical, that is, N_T and N_S increase with increasing R_T. Along this oscillatory branch the period of the oscillation increases monotonically because of the increasing influence of the temperature field. Expressed in terms of the typical fluid particle, the explanation is that during its oscillatory displacement, the particle experiences a restoring force which decreases as R_T increases, and hence the period increases. Figure 5 presents a typical plot of N_T and N_S against time for one value of σ, τ, R_T and R_S. The phase delay of N_S with respect to N_T is clearly seen. This delay occurs because the salt field diffuses more slowly than the temperature field. The slower diffusion of salt is also the reason why both the mean and the range of N_S are larger than those of N_T.

As R_T increases, this form of motion continues until R_T reaches a specific value, R_2, say. At $R_T = R_2$ the motion changes in form. Either the motion becomes time-independent, a situation discussed below, or in the more general case, the motion develops a further structure as is indicated in the form of N_T or N_S as a function of time, as graphed in Fig. 6. In both N_T and N_S there are four extrema, two maxima and two minima, per period, where the period is defined in the usual sense as the time between two identical states. As seen in Fig. 6, the time between the smaller maximum and the preceeding larger maximum is greater than the time between the smaller maximum and the following larger maximum. This holds for both N_T and N_S. As R_T increases above R_2, these times evolve continuously from the single period exhibited by N_T or N_S for R_T just below R_2. This form of motion is due to the increasing temperature difference attempting to induce monotonic motion. Fluid near one of the lower corners of the cell rises, sinks by a different route, rises by a smaller amount in an attempt to readjust the form of motion, sinks again, and the total form of motion is then repeated. Other fluid particles in the cell move accordingly. This form of motion occurs until $R_T = R_3$, say, at which value a transition either to a time-independent solution or, more generally, a disordered non-periodic form of motion occurs.

No motion with three, four or more maxima per cycle was found for the values of σ, τ, R_T or R_S examined.

Non-periodic motion continues to exist at increasing R_T until for $R_T = R_4$, say, an equilibrium time-dependent solution can no longer be maintained and the only equilibrium solutions are time-independent. For some values of σ, τ and R_S this time-independent form occurs before the solution passes through the two-maxima-per-cycle form of motion or the non-periodic form.

For future use we denote by R_4' the value of R_T at which the transition to an equilibrium time-independent solution occurs.

The Monotonic Branch

For all $R_T > R_4'$ monotonic motion ensues. Such a form of motion exists in a double-diffusive fluid because the temperature field can produce an almost isosaline core, with all salinity gradients confined to boundary layers, thinner than the thermal boundary layers by an amount $\tau^{\frac{1}{2}}$. In these salinity boundary layers, the effect of the stabilizing salinity gradient on the temperature field is arrested because of the different diffusivities. For sufficiently high R_T, the destabilizing temperature effects can thus overcome the restoring effects of the salinity. This steady form of motion is a very efficient way of transporting heat and salt and thus the equilibrium Nusselt numbers undergo a discontinuous increase as the solution changes from the oscillatory branch to the monotonic branch.

Gradually decreasing R_T from some value greater than R_4' the equilibrium monotonic motions retrace the states that would have been obtained on increasing R_T from R_4' ; thus there is a unique stable equilibrium solution for $R_T > R_4'$.

Decreasing R_T below R_4' an equilibrium monotonic solution continues to exist, with decreasing Nusselt numbers, until $R_T = R_5$, say. Further decrease of R_T leads to a solution on the oscillatory branch already described, or, if $R_5 < R_1$, to conduction. There is thus a hysteresis between these two different modes of motion.

The non-linear monotonic branch emanates from the bifurcation point at $R_T = R_6$ and the behaviour of the solution about $R_T = R_6$ can be obtained by using standard perturbation procedures. Results obtained by this method indicate that R_6 is a subcritical bifurcation point, that is, N_T and N_S increase with decreasing R_T . The results also indicate that solutions on the branch are unstable to time-dependent two-dimensional disturbances until the branch passes through a minimum value of R_T , that is, until the branch passes through $R_T = R_5$. Thereafter, the branch continues, and is stable, with the amplitude of the motion increasing as R_T increases.

The Interaction Between The Oscillatory And Monotonic Branches

As is evident from the Table, the oscillatory and monotonic branches take quite different relative positions depending upon the values of σ, τ and R_S . The influence of these parameters can be summarised as follows. The linear monotonic mode is independent of σ because fluid particles undergoing monotonic linear motion conserve their momentum. Along the non-linear part of the monotonic branch the motion is only weakly dependent upon σ, just as in purely thermal convection (10,11). By contrast, the motion on the oscillatory branch is quite dependent upon the value of σ because the magnitude of the phase delay between the temperature and displacement field, which drives the motion, is determined by σ . The relative influence of τ is almost exactly the opposite. The whole monotonic branch is strongly dependent on the magnitude of τ because its value indicates how slowly the salt field diffuses and hence how effectively the salt field can overcome the tendency of the temperature field to drive steady convection. However, along the oscillatory branch the value of τ determines the phase lag between the salinity and temperature field, a lag which has only a small influence on the motion. The value of R_S , which indicates the magnitude of the stabilising salt field, has a large influence on both branches.

The various different orientations of the two branches and the hysteresis loop that connects them are summarised in the Table. Of particular interest is the value of R_5 , the minimum thermal Rayleigh number for which (non-linear) monotonic convection is possible. Upper and lower bounds to R_5 for various values of σ, τ and R_S are presented in the Table and Figs 1-3.

Consider first Fig. 1, which presents the bounds to R_5 for $\sigma = 1, \tau = 10^{-\frac{1}{2}}$ and various values of R_S . For each of these values, R_5 is greater than R_1 and only for the largest value of R_S is R_5 less than R_S .

Decreasing τ to 10^{-1} without altering σ , we obtain the results plotted in Fig. 2. The four ranges for R_5 are, as expected, all less than those for $\tau = 10^{-1}$. For $R_S = 10^3$ and $R_S = 1.5 \times 10^3$, R_T is less than R_S .

The ranges of R_5 for $\sigma = 10$ and $\tau = 10^{-1}$ are plotted in Fig. 3. For $R_S = 10^3$, R_5 is less than R_1 , but due to the relatively large viscous dissipation at these small Rayleigh numbers $R_5 > R_S$. For $R_S = 10^4$ or 1.5×10^4 , R_5 is less than both R_1 and R_S . Thus for these values of σ, τ and R_S, (non-linear) steady convection can occur when the fluid is statically stable and linear theory predicts the existence of only a conduction solution.

CONCLUSIONS

The major conclusions of the study reported in this paper are as follows. Non-linear equilibrium solutions of the double-diffusive Benard problem belong to one of two branches. One is an oscillatory branch, which emanates from the linear steady-state oscillatory solution. As R_T is increased, the solutions along this branch alter in such a way that the associated Nusselt numbers change from one maximum per period (Fig. 5), to two maxima per period (Fig. 6), to a non-periodic state. The other branch is composed of monotonic solutions, which emanate sub-critically from the linear steady-state monotonic solution. Solutions on this branch are unstable until the branch passes through its minimum value of R_T , following which the solutions are stable - at least in two dimensions. Stable solutions on both branches can exist at the same values of R_T , R_S , σ and τ. This leads to a hysteresis effect if solutions obtained from increasing R_T and then decreasing R_T are followed. Depending upon the value of σ, τ and R_S , as R_T increases, instability may first occur as an oscillatory mode or a non-linear monotonic mode. The existence of a non-periodic solution that evolves into a time-independent form above a critical value of R_T indicates that by <u>increasing</u> R_T disordered motion can be suppressed.

ACKNOWLEDGEMENTS

It is a pleasure to acknowledge the help of Dr. D. R. Moore and Dr. J. M. Wheeler in carrying out the numerical calculations reported in this paper.

NOMENCLATURE

D	plate separation
g	gravity
L	horizontal size of convection cell
N_T	thermal Nusselt number
N_S	saline Nusselt number
q^*	velocity vector
R_T	thermal Rayleigh number
R_S	saline Rayleigh number
$R_1 - R_6$	critical thermal Rayleigh numbers

R_C	a particular thermal Rayleigh number
R_X	a particular saline Rayleigh number
S^*	salinity
S_o	reference salinity
S	disturbance salinity
T^*	temperature
T_o	reference temperature
T	disturbance temperature
x	horizontal co-ordinate
z	vertical co-ordinate
α	thermal expansion coefficient
β	saline expansion coefficient
ΔS	salinity difference between plates
ΔT	temperature difference between plates
δt	time step
κ_S	saline diffusivity
κ_T	thermal diffusivity
ν	kinematic viscosity
ρ^*	density
ρ_o	reference density
σ	Prandtl number
τ	κ_S/κ_T
ψ	streamfunction

REFERENCES

1. Turner, J. S. Double-diffusive phenomena, Ann. Rev. Fluid Mech., 1974, 6, 37-56.

2. Stern, M. E. The 'salt-fountain' and thermohaline convection, Tellus, 1960, 12, 172-5.

3. Straus, J. M. Finite amplitude doubly diffusive convection, J. Fluid Mech., 56, 353-74.

4. Spiegel, E. A. Convection in stars. I Basic Boussinesq convection. Ann. Rev. Astron. and Astrophys., 1971, 9, 323-52.

5. Huppert, H. E. and P. C. Manins. Limiting conditions for salt-fingering at an interface. Deep-Sea Res., 1973, 20, 315-23.

6. Veronis, G. Effect of a stabilizing gradient of solute on thermal convection. J. Fluid Mech., 1968, 34, 315-36.

7. Baines, P. G. and A. E. Gill. On thermohaline convection with linear gradients. J. Fluid Mech., 1969, 37, 289-306.

8. Turner, J. S. Buoyancy effects in fluids. Cambridge, England: Cambridge University Press, 1973.

9. Moore, D. R., R. S. Peckover and N. O. Weiss. Difference methods for time-dependent two-dimensional convection. Computer Phys. Commun., 1973, 6, 198-220.

10. Veronis, G. Large-amplitude Benard convection. J. Fluid Mech., 1965, 26, 49-68.

11. Moore, D. R. and N. O. Weiss. Two-dimensional Rayleigh-Benard convection. J. Fluid Mech., 1973, 58, 289-312.

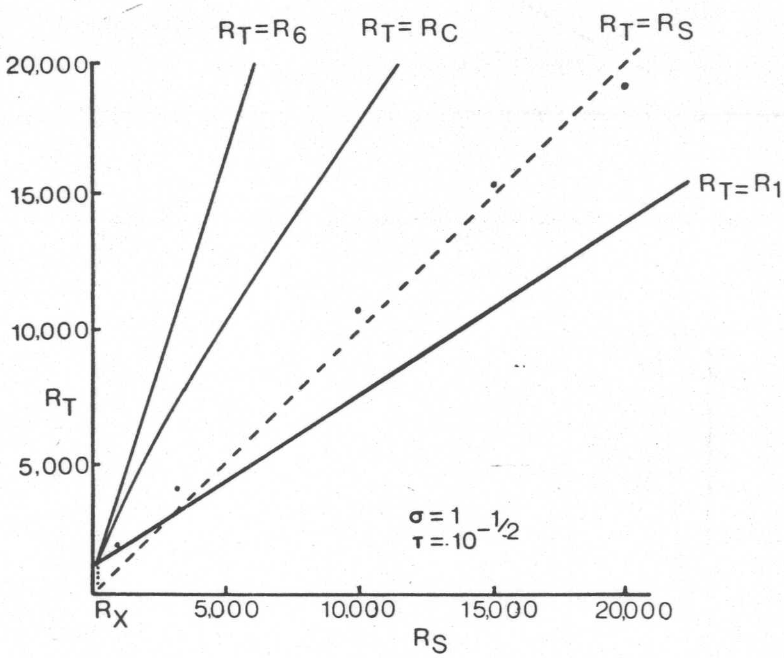

Fig. 1 The stability boundaries of linear theory and the minimum R_T for stationary monotonic convection. According to linear theory, on $R_T = R_1$ an oscillatory mode is initiated, on $R_T = R_C$ this mode becomes a purely growing exponential, and on $R_T = R_6$ there is a time-independent mode. The straight lines $R_T = R_1$ and $R_T = R_6$ meet at $R_S = R_X$.

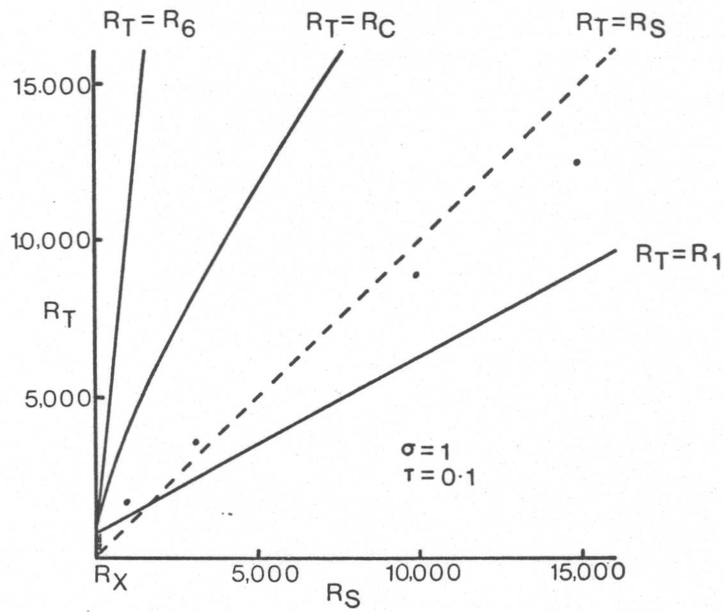

Fig. 2 As for Fig. 1 except that $\tau = 0.1$.

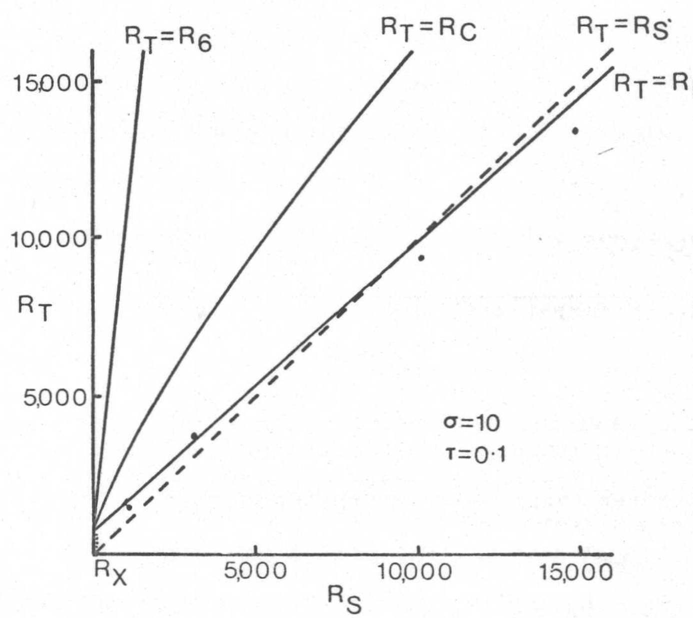

Fig. 3 As for Fig. 2 except that $\sigma = 10$.

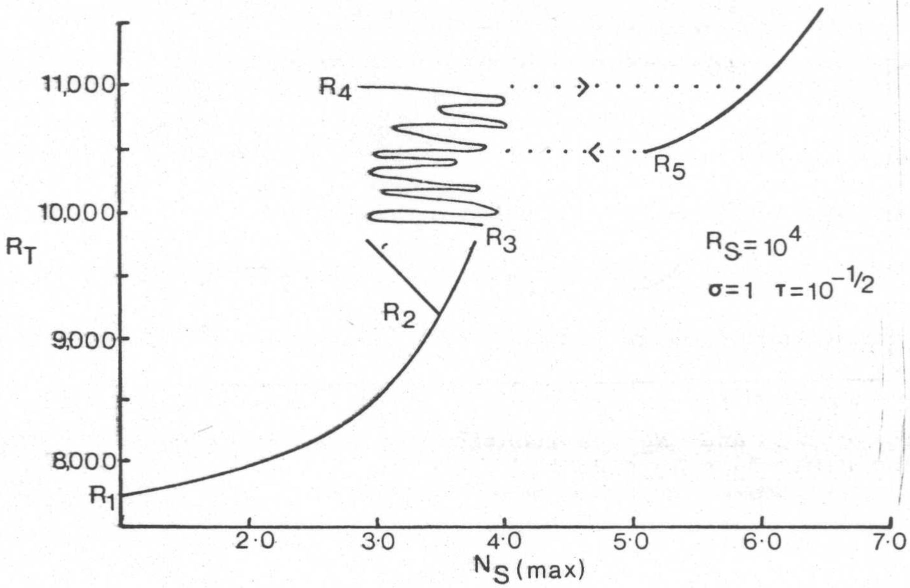

Fig. 4 The maximum value of N_S as a function of R_T for stable equilibrium convection. For $R_2 < R_T < R_3$, N_S has two local maxima per period and both are shown. For $R_3 < R_T < R_4$ the motion is non-periodic.

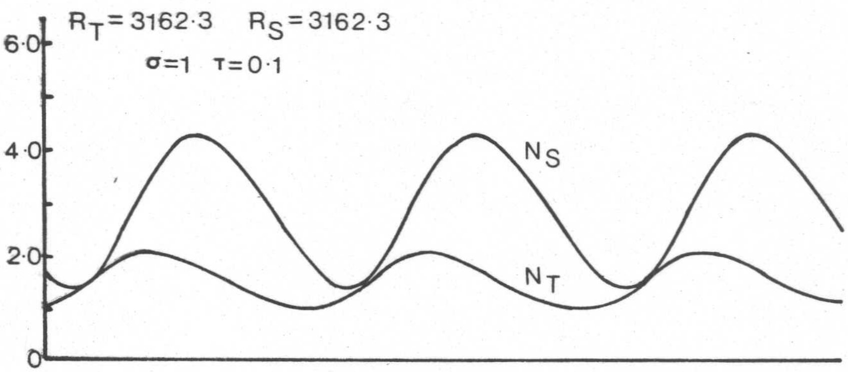

Fig. 5 N_T and N_S as functions of time for a typical case with $R_1 < R_T < R_2$.

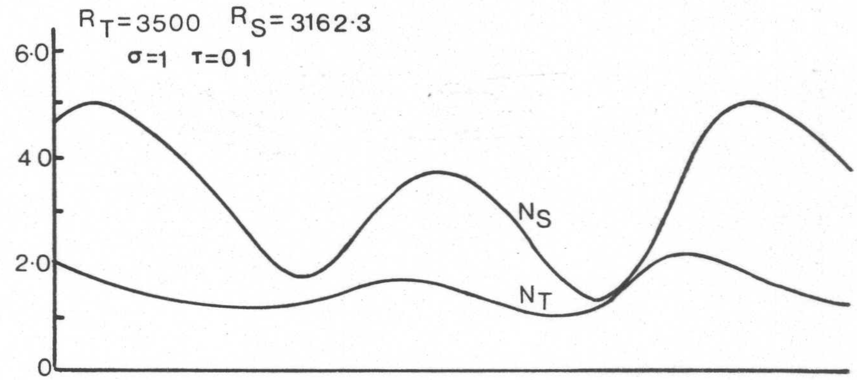

Fig. 6 N_T and N_S as functions of time for a typical case with $R_2 < R_T < R_3$.

σ	τ	R_S	R_1	R_4'	R_5	R_6
1.0	0.316	1,000	1,797	2,200-2,300	2,000-2,100	3,820
1.0	0.316	3,162	3,220	4,400-4,500	4,100-4,200	10,658
1.0	0.316	10,000	7,720	11,000-11,200	10,400-10,500	32,280
1.0	0.316	15,000	11,010	15,600-15,800	15,000-15,200	48,092
1.0	0.316	20,000	14,301		19,400-19,600	63,903
1.0	0.1	1,000	1,346	1,900-2,000	1,700-1,800	10,658
1.0	0.1	3,162	2,535	4,100-4,200	3,500-3,600	32,280
1.0	0.1	10,000	6,296	10,000-10,200	8,800-9,000	100,658
1.0	0.1	15,000	9,046		12,300-12,700	150,658
10.0	0.1	1,000	1,831		1,700-1,800	10,658
10.0	0.1	3,162	3,634		3,700-3,800	32,280
10.0	0.1	10,000	10,271		9,300-9,600	100,658
10.0	0.1	15,000	14,961		13,400-13,700	150,658

The values of R_1, R_4', R_5 and R_6 for various σ, τ and R_S. At $R_T = R_1$ linear theory predicts the onset of oscillatory convection; R_4' is the largest value of R_T for which stable time-dependent motion is possible; R_5 is the smallest value of R_T for which monotonic motion is possible; and at $R_T = R_6$ linear theory predicts steady monotonic motion.